Solar Physics
DOI: 10.1007/•••••-•••-•••-••••-•

Kilometric type II radio emissions in Wind/WAVES TNR data and association with interplanetary structures near Earth

Franco Manini[1]•• · Hebe Cremades[1]•• · Fernando M. López[1]•• · Teresa Nieves-Chinchilla[2]••

Abstract Type II radio bursts arise as a consequence of shocks typically driven by coronal mass ejections (CMEs). When these shocks propagate outward from the Sun, their associated radio emissions drift down in frequency as excited particles emit at the local plasma frequency, creating the usual Type II patterns. In this work, we use dynamic spectra from the Wind/WAVES Thermal Noise Receiver (TNR) to identify Type II radio emissions in the kilometric wavelength range (kmTIIs, $f < 300$ kHz) between 1 January 2000 and 31 December 2012, i.e. over a solar cycle. We identified 134 kmTII events and compiled various characteristics for each of them. Of particular importance is the finding of 45 kmTII events not reported by the official Wind/WAVES catalog (based on RAD1 and RAD2 data). We search for associations with interplanetary structures and analyze their main characteristics, in order to reveal distinctive attributes that may correlate with the occurrence of kmTII emission. We find that the fraction of interplanetary coronal mass ejections (ICMEs) classified as magnetic clouds (MCs) that are associated with kmTIIs is roughly similar to that of MCs not associated with kmTIIs. Conversely, the fraction of ICMEs with bidirectional electrons is significantly larger for those ICMEs associated with kmTIIs (74 % vs. 48 %). Likewise, ICMEs associated with kmTIIs are on average 23 % faster. The disturbance storm time (DsT) mean value is almost twice as large for kmTII-associated ICMEs, indicating that they tend to produce intense geomagnetic storms. In addition, the proportion of ICMEs producing moderate to intense geomagnetic storms is twice as large for the kmTII-associated ICMEs. After this investigation, TNR data prove to be valuable not only as complementary data for the analysis of kmTII events but also for forecasting the arrival of shocks at Earth.

✉ F. Manini
franco.manini@um.edu.ar

[1] Universidad de Mendoza, CONICET, Grupo de Estudios en Heliofisica de Mendoza, Boulogne Sur Mer 665 (5 500) Mendoza, Argentina

[2] Heliospheric Physics Laboratory, Heliophysics Science Division, NASA Goddard Space Flight Center, 8800 Greenbelt Rd., Greenbelt, MD 20770, USA

Keywords: Radio Bursts, Type II; Solar Wind, Shock Waves; Coronal Mass Ejection, Interplanetary; Radio Bursts, Dynamic Spectra

1. Introduction

Observations in the radio frequency domain provide an important source of information about physical processes that take place in the solar corona and the heliosphere. Of particular interest are the radio observations in the low frequency range, from metric (300-30 MHz) to kilometric wavelengths (f < 300 kHz). It is in this frequency interval where it is possible to observe type II radio bursts (Wild and LL., 1950; Wild, Murray, and Rowe, 1954). Radio emissions associated to type II bursts are believed to originate in the upstream regions of magneto-hydrodynamic (MHD) shocks mostly driven by coronal mass ejections (CMEs) propagating outward in the solar corona and the interplanetary medium (Reiner et al., 1997; Bale et al., 1999).

During its propagation in the heliosphere, a CME-driven shock encounters a plasma density that decreases with increasing heliocentric distance. As the type II emission frequency is directly related with the local plasma density, the outward-propagating shock gives rise to an emission pattern that drifts down to lower frequencies as time (and distance) progresses (Reiner et al., 1997). The frequency of radio bursts can give a rough estimation of the heliocentric distance (R) at which it is produced (e.g. Leblanc, Dulk, and Bougeret, 1998). Although the generation mechanism of Type II bursts is to date not fully understood, they can be regarded as electrons undergoing shock-drift acceleration and developing a beam distribution of reflected electrons at shocks. This enables growth of Langmuir waves via the beam instability in the upstream foreshock, while Langmuir wave energy is converted into radio emission near the electron plasma frequency and its harmonic, via nonlinear wave-wave processes (Knock et al., 2001; Chernov and Fomichev, 2021). Dynamic spectra (DS) thus constitute a valuable resource to visualize these drifting emissions among other radio phenomena (Reiner et al., 1998).

Observations below 300 kHz can be used to detect the signal from type II bursts emitted at kilometric wavelengths (hereafter kmTII), which correspond to distances roughly beyond 20 solar radii ($R_\odot$) and all the way down to 1 AU. Particularly for the case of long-wavelength Type IIs, it is worth mentioning that the fact that they extend to such low frequencies is indicative that the shock must still be highly energetic at large distances to keep the plasma emission mechanism energized, turning kmTIIs into a valuable and special asset. Also, according to Corona-Romero et al. (2015), all the interplanetary shock waves associated with kmTIIs are explosive beyond 20 $R_\odot$.

The first report of a kmTII was made in 1973 (Malitson, Fainberg, and Stone, 1973). Later, in 1982, Cane, Stone, and Fainberg (1982) identified several kmTII events using data from ISEE-3. Cane, Sheeley, and Howard (1987) found that kmTII bursts were associated with the most energetic and massive CMEs observed by the Solwind coronagraph. A major advance in radio observations at low frequencies came with the launch of the Wind mission, in particular with the instrument Radio and Plasma Wave Experiment (WAVES, Bougeret et al., 1995). The use of data provided by WAVES has allowed the analysis of plasma emission from type II bursts from the solar corona to the Earth environment (e.g., Cane and Erickson, 2005; Gonzalez-Esparza and Aguilar-Rodriguez, 2009a; Hillan, Cairns, and Robinson, 2012; Xie et al., 2012). More specifically, the

Wind/WAVES receiver RAD2 (Radio Receiver Band 2; 1-14 MHz) can be used for the detection of type II events in the metric-decametric wavelength range, while RAD1 (Radio Receiver Band 1; 20-1040 kHz) can be used for those in the hectometric-kilometric range. Such list of events detected by these two receivers has been compiled and made available online in the Wind/WAVES official website[1] as a "Possible Type II and IV Radio Bursts Observed by WIND/WAVES" (hereafter "Wind list"). RAD1 and RAD2 data have been intensively used to analyze type II radio bursts (e.g., Kaiser et al., 1998; Dulk, Leblanc, and Bougeret, 1999; Reiner, Kaiser, and Bougeret, 2007; Gopalswamy, Mäkelä, and Yashiro, 2019).

The Thermal Noise Receiver (TNR; 4-256 kHz), is also part of the Wind/WAVES instrument suite. Efforts dealing with TNR data (e.g., Gonzalez-Esparza and Aguilar-Rodriguez, 2009b; Aguilar-Rodriguez, Gonzalez-Esparza, and Ontiveros, 2010) are scarce in comparison to those using the other Wind/WAVES detectors. Although RAD1 and TNR may appear to largely overlap in frequency, the latter has a much higher spectral resolution, which turns it into a valuable asset for the detection and analysis of kmTII events. Taking advantage of TNR's capabilities, Cremades, St. Cyr, and Kaiser (2007) developed a technique to estimate the speed of shocks based on the associated kmTII emission. In a similar way, Cremades et al. (2015) analyzed 71 Earth-directed shocks driven by CMEs to predict their arrival time at 1 AU. These papers remark the importance of using kmTII emission for tracking CMEs in the interplanetary medium (ICMEs), a fundamental aspect in space weather forecasting. Nonetheless, a complete survey of kmTII radio emissions identified in the Wind/WAVES TNR data and their association with interplanetary (IP) structures has not been carried out to date. This is a crucial step towards understanding which characteristics of IP structures are prone to result in kmTII emissions. Moreover, the geoeffectiveness of IP structures associated to kmTII emissions can be assessed to acknowledge for differences with respect to those not associated to kmTII emissions. Through the analysis of TNR DS, here we present the results of a careful survey in which we compiled a list of 134 kmTII events. These events were subsequently associated with interplanetary transient events detected in-situ at Earth-L1, such as shocks and ICMEs.

The manuscript is organized as follows. In Section 2 we describe the methodology used to identify the kmTII events. In Section 3 we explain the procedure followed to associate the IP structures detected in situ at 1 AU with our kmTII events. In Section 4 we summarize the results concerning statistics, characteristics of associated ICMEs and geoeffectiveness. Finally, in Section 5 we summarize our findings and discuss their implications. The complete table of identified events can be found in the Appendix at the end of the manuscript.

2. Identification of the kmTII events

In this section we present the procedure used to identify the kmTII events using data from the Wind/WAVES TNR radio receiver, and the compiled list of events. The access to the Wind data is open and performed through the Wind/WAVES official website as mentioned above.

[1] https://solar-radio.gsfc.nasa.gov/wind/data_products.html

To identify the kmTII events, we generate DS from the signal detected by TNR. For the purpose of this analysis, we built DS that display the radio emission in the inverse frequency domain (f^{-1}) as a function of time (see sample DS in Figure 1). We prefer to use f^{-1} because the average IP plasma density varies as $1/R^2$, and the plasma frequency $f\,[kHz]$ is proportional to the electron density $n_e[\,\mathrm{cm}^3]$ by $f \propto \sqrt{n_e}$, the plasma frequency scales as $1/R$, thus $1/f$ scales as R (Reiner et al., 1997). An emission observed in a DS is considered as a kmTII event if the two following conditions are met: i) it shows a substantial decay in frequency, of at least 0.5 kHz per hour (In the $1/f$ domain, this approximately equals to 0.00133 kHz^{-1} per hour) and ii) the emission is observed in the DS in connection with an eruption previously occurred, related to its origin in the low solar corona. A typical signature associated with an eruption is a Type III radio burst, but if the latter is not present, the eruption can be identified in e.g. Extreme Ultraviolet (EUV) imagery of the low corona.

In Figure 1 we show a DS that exemplifies the conditions described above. The figure displays a case of type II radio emission occurred during the rising phase of solar cycle 24, with the upper panel corresponding to RAD1 frequencies and the lower panel to TNR. Type II radio emission can be discerned in both DS, with an improved resolution in frequency for the case of TNR. In the TNR panel, the kmTII is delimited by the red dashed lines that meets both aforementioned conditions. A type III radio burst can be seen in both DS, in association with the start of the event. In the lower frequency region of the lower panel, it is possible to observe the plasma frequency line (PFL) as a wandering continuous emission at all times. A shock wave can also be noticed where the red dashed lines end, at 14:40 GMT on 24 January. The shock arrival produces a sudden increase in the frequency of the emission associated with the PFL, due to the shock density enhancement.

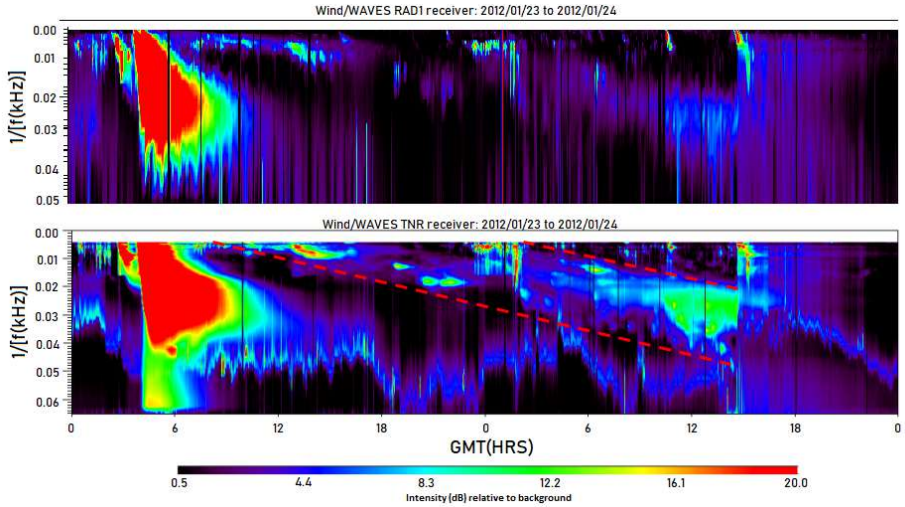

Figure 1. DS showing the radio emission detected by RAD1 (upper panel) and TNR (lower panel) during 23 and 24 of January 2012. The emission between the red dashed lines in the lower panel is a clear kmTII event observed during those days, that has also left an imprint in the RAD1 DS. The upper panel covers the range of frequencies 1040-20 kHz, and the lower panel 256-15 kHz.

Our investigation uses 12 years of data, from 1 January 2000 to 31 December 2012, thus partially covering solar cycles 23 and 24. From the analysis of all DS during that time interval, we could identify 134 kmTII events. All 134 compiled events are listed in Table 3, together with their main characteristics and associated interplanetary structures. While the radio events themselves are introduced in this section, the properties of the associated shocks and ICMEs are described in Section 3. The list is also available for download at https://sites.google.com/um.edu.ar/gehme/science/km-tii-catalogue.

The first group of columns 'KmTII' (1-5) in the table displays information on the identified kmTII events: start date and time, end date and time, and frequency range in kHz. It is important to remark that we could not find any kmTII event during the years 2008, 2009 and 2010. The column 'Wind/WAVES' (6) in Table 3 lists the related events that are reported by the Wind list using the same reference number of the event as listed, following the corresponding year. Those events without reference number in this column, are kmTII events identified by us, that are not reported by the Wind list. The procedure of association of each identified kmTII in the DS of TNR with a counterpart registered in the official Wind list, required two conditions that must be simultaneously met: i) There must be a temporal agreement between both entries and ii) The lower limit in frequency of the emission reported by the Wind list should extend beyond the upper limit of TNR's frequency detection range. It is worth noting that there are events which had been catalogued in the Wind list as reaching down to TNR frequencies but not observed in the DS of TNR, therefore not considered in our analysis.

The second group of columns 'In situ shock' displays information on the association with shocks detected by the Wind and/or ACE spacecraft. The third group of columns 'ICME' summarizes the main characteristics of the associated ICMEs. These two groups of columns will be addressed in detail in Section 3.

3. Association between kmTII and interplanetary transient phenomena detected in-situ at 1 AU

Once the kmTII events are identified in the DS of TNR, we searched for their spatial and temporal association with interplanetary transient structures detected in-situ at the Earth's environment. To accomplish this task we used data available from several online catalogs, as described below.

In the case of interplanetary shocks, we used the database compiled by the Harvard-Smithsonian Center for Astrophysics (CfA[2]) which is based in data from the Wind and the Advanced Composition Explorer (ACE) spacecraft. Alternatively, we used the "List of disturbances and transients" compiled by the University of New Hampshire (UNH[3]).

As mentioned above, kmTIIs typically correspond to distances beyond $20\,R_\odot$ and all the way down to 1 AU. The average starting frequency of the kmTIIs identified in this study is 185 kHz ($\approx 33\,R_\odot$), while they typically end at 54 kHz ($\approx 117\,R_\odot$). This poses them as a valuable resource to predict shock arrival times in advance. Having said this, to associate a kmTII to an interplanetary shock, we considered as possible

[2] https://www.cfa.harvard.edu/shocks/

[3] http://www.ssg.sr.unh.edu/mag/ace/ACElists/obs_list.html

candidates those shocks detected no more than four days since the beginning of the kmTII emission. This criterion is an upper limit assuming that a CME traveling at 400 km s^{-1} would take approximately that amount of time to reach 1 AU. If more than one shock is registered within such time interval, we examined the DS following the procedure described in Cremades, St. Cyr, and Kaiser (2007): to find the most likely associated shock, we used a linear fit to extrapolate forward in time the kmTII emission which should intersect the abrupt signal increment of the PFL given by the arrival of the respective shock at 1 AU. Then, the intersection time of the fit is compared with the in-situ arrival time provided by the shock catalogs. The CfA Wind shock catalog was always consulted first. In those cases where we could not associate any shock reported there, we conducted the search in the CfA ACE and UNH shock databases.

The result of following this association procedure is displayed in the second group of columns in Table 3 (In situ shock). Columns 7 to 10 display information about the start date and time for the shocks locally detected by the Wind and/or ACE spacecraft, median shock speed, and the catalog used to extract that information. The blank spaces indicate that we could not associate any shock to the corresponding kmTII event. In this respect, it is worth noting that even though we assume for a first approximation that observing a kmTII with Wind/WAVES implies that the shock/CME is Earth directed, this might not necessarily be the case. These radio emissions are widely beamed, thus they can be detected at a particular location (i.e. Wind) without implying that the shock is actually traveling in that direction. That is, the solid angle through which kmTII associated shocks/CMEs can be emitted such that they intersect L1 is smaller than the solid angle through which they can be emitted and their radio emission be detected at L1. Therefore, it is highly likely that for several detected kmTII, we will not be able to observe their associated shocks. See section 5 for additional discussion regarding this subject.

To study the association between the identified kmTII events and the observed ICMEs, we use the following catalogs of ICME transient events: The Richardson-Cane list (Cane and Richardson, 2003; Richardson and Cane, 2010, hereafter RC[4]), using the ACE spacecraft, and the one compiled by Teresa Nieves-Chinchilla (Nieves-Chinchilla et al., 2018, 2019, hereafter TNC[5]), using the Wind spacecraft.

In our analysis, we assume that an ICME is related to the kmTII, if such ICME starts right after a cataloged interplanetary shock, and/or within a four-day period since the kmTII start. For those cases without shock association, the kmTII profiles were linearly projected down to the PFL to have a proxy of the date and time of arrival, so as to enable an ICME association in RC and/or TNC catalogs.

The third group of columns (11-19) in Table 3 summarize the main characteristics of the associated ICMEs. Columns 11 and 12 identify the start date and time of the ICMEs that we could associate with our kmTII events. Column 13 (“MC”) indicates the classification used in RC (described in Cane and Richardson, 2003; Richardson and Cane, 2010) with regards to a magnetic cloud (MC): “0” means no detection of MC, “1” some characteristics are present but lacks rotation or enhanced magnetic field, and “2” all MC requirements are fulfilled. Column 14 (“MO”, for magnetic obstacle) indicates the

[4] http://www.srl.caltech.edu/ACE/ASC/DATA/level3/icmetable2.html

[5] https://wind.nasa.gov/ICME_catalog/ICME_catalog_viewer.php

type of magnetic structure according to TNC (as described in Nieves-Chinchilla et al., 2018, 2019): “Fr” flux rope, “F+” or “F-” flux rope with large or small rotation respectively, “Cx” Complex, and “E” Ejecta. Column 15 (“BDE”) indicates the presence of bidirectional electrons in ACE/SWEPAM observations according to RC. When ’SEP’ appears, it means that a storm was in progress so it could not be determined. Column 16 (V_{ICME}) presents the mean ICME speed, based on solar wind speed observations during the period of the passage of the ICME, in the RC catalogue. For those events catalogued only in the TNC catalogue, this value corresponds to the mean solar wind bulk velocity (V_{sw} in that table) in the Magnetic Object interval. Column 17 (“B”) is the mean magnetic field strength in the ICME. When only the TNC catalog is used, the value is for the MO interval. Column 18 shows the disturbance storm time index (DsT) associated with the corresponding ICMEs after their arrival to Earth. For those cases where the corresponding ICMEs were only listed in the TNC catalog, we estimated the corresponding DsT values manually[6]. To this end, we followed the same criteria used in the RC list, namely taking the minimum value reported by the World Data Center for Geomagnetism, Kyoto[7] during the ICME duration interval. The last column, 19, indicates the catalog (RC and/or TNC) used to extract the ICMEs information in every case. Blank spaces indicate that no ICME from the catalogs could be associated with the respective kmTII event.

4. Results

4.1. Statistical analysis of the identified events

A summary of the resulting associations between kmTII events and interplanetary structures detected in situ is displayed in Table 1. Based on the analysis of TNR data, we could identify 134 kmTII radio emission events, out of which 45 (33%) are not listed in the Wind’s list, i.e. these events were not reported on the basis of data from RAD1 and/or RAD2.

From the total number of events, 77 (57%) could be associated to an interplanetary shock, hence 57 kmTII emission events were not. It is worth noting that for the 89 kmTIIs that were reported by the Wind’s list, 54 (61%) can be associated with interplanetary shocks, while this number is 23 (51%) for those not previously reported. Furthermore, 62 events (47%) out of the total amount of kmTIIs could be associated with an ICME, while the proportion is practically the same for the subsets of events previously reported by the Wind’s list and those that were newly identified in this work. In the same way, the relationships between the amount of events with ICMEs and MCs, with and without shockwaves, is similar between our list and the Wind list.

To examine the variation with the solar cycle, we display in Figure 2 the total number of kmTII events compiled per year, as well as how many of them could be associated to an interplanetary shock and to both, a shock and an ICME. The figure indicates that for years 2000 to 2002 the ratio of kmTII events with associated shock waves is

[6]As a consequence of this work, we provided the TNC catalog with DsT values for all their entries. See acknowledgments in https://wind.nasa.gov/ICMEindex.php.

[7]https://wdc.kugi.kyoto-u.ac.jp/dst_final/index.html

Table 1. Number of identified kmTII events and their association with in-situ interplanetary structures.

	All	Prev. reported	Newly reported
KmTII events	134	89	45
With shockwave	77	54	23
With ICME	62	42	20
With shock and ICME	51	35	16
With shock - No ICME	26	19	7
With ICME - No shock	11	6	5

significantly larger than 50% with respect to the total amount of kmTII events, thus corresponding to the period of maximum activity of solar cycle 23. For year 2003, this ratio is considerably lower, while for years 2004 – 2006 and 2011 – 2012 the proportion is around 50%. Besides, when considering the number of kmTII events associated with both, shocks and ICMEs, the ratio with respect to the total of kmTII events is lower than 50% for every year, except for 2002 when it is significantly larger. The fact that this fraction is not roughly constant over the solar cycle, as it would be expected if only the larger beam width vs. the shock extent (Section 3) is responsible for the difference, suggests that other mechanisms might be at work (see Section 5). The yearly number of all shocks reported by Wind and ACE, and all ICMEs reported by RC and TNC are shown for reference in dashed-dotted and dashed lines respectively. The yearly number of shocks (from both CfA Wind and ACE catalogs) arises from considering all shock events, counting only once those that are duplicated in the catalogs. The same procedure was applied to compile the yearly number of ICMEs, arising from the RC and TNC catalogs.

4.2. Comparison of ICMEs with and without associated kmTII

In view to understand if there are intrinsic differences between ICMEs associated with kmTII (kmTII-ICMEs) and those that are not (other-ICMEs), here we compare the properties of both ICME groups. As mentioned in Table 1, the kmTII-ICMEs group is comprised of 62 events. The procedure to compile the other-ICMEs group is as follows: As a starting point, we compiled a joint list of ICMEs from both TNC and RC catalogues during the investigated time period (2000-2012), and removed those entries associated with kmTIIs. Every event was carefully checked to have been computed only once in the merged other-ICMEs list, which is finally comprised of 302 cases.

To characterize both of the ICME groups, we consider the following aspects: MC, BDE and V_{ICME}. These properties were described in Section 3, while the respective values corresponding to the group kmTII-ICMEs are presented in columns 13, 14, 15 and 16 of Table 3. With regards to the MC aspect, it becomes necessary to reconcile the classification used by the TNC and RC catalogues. We associate the TNC classification (E, Cx, F; Table 3, column 14) with that of RC (0, 1, 2; Table 3, column 13), by assuming E=0, Cx=1 and F=2. The results of this analysis are summarized in Table 2.

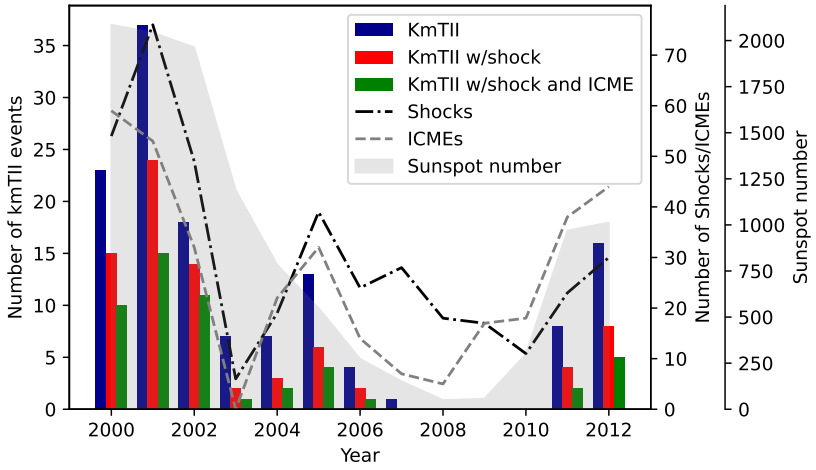

Figure 2. Yearly frequency of identified kmTIIs (blue), kmTIIs with associated shocks (red), and kmTIIs associated with both, a shock and an ICME (green). The yearly number of shocks and ICMEs are shown in black and grey lines respectively. The scales of the primary and secondary y-axes differ by a factor of 2, given that the number of shocks/ICMEs almost double the number of kmTIIs. The gray shaded area represents the yearly sunspot number and its scale is in the tertiary axis.

Our study indicates that the fraction of ICMEs classified as MCs is quite similar for the cases where the events were and were not associated with kmTII emission, resulting in 21 out of 62 (34%) and 118 out of 302 (39%) events respectively.

The comparison of the detection of BDEs does show a remarkable difference between both groups (see second row of Table 2). For the kmTII-ICMEs group, the number of events which present BDEs is of 46 out of 62 (74%), while for the other-ICMEs group the proportion is 145 out of 302 (48%), which is significantly lower.

In Figure 3 we show histograms of V_{ICME} for both analyzed groups. The mean values of V_{ICME} in Table 2 indicate that on average, the events of the kmTII-ICMEs group are around 23% faster than those without evidence of kmTII. The median values are 515 km s^{-1} and 420 km s^{-1} respectively, also supporting the large difference between both groups. This result is in agreement with the recent findings of Patel et al. (2022). They compare the mean values of V_{ICME} for ICMEs detected during solar cycles 23 and 24, associated and not associated with decametric and hectometric type II radio emission, finding similar values to those of our study. Also, Gopalswamy et al. (2008) found that metric and kilometric type II bursts are associated with CMEs with higher average speeds.

4.3. Geoeffectiveness of ICMEs with and without associated kmTII

Of particular interest is the analysis of the geoeffectiveness resulting from the arrival of ICMEs which present kmTII emission and from those that do not. With this objective, we consider the same groups, kmTII-ICMEs and other-ICMEs, introduced in Section 4.2.

In order to quantify geoeffectiveness we use the DsT index (see Section 3). The mean Dst for the kmTII-ICMEs group yields -111, while that of the other-ICMEs group is -

Table 2. Proportion of ICMEs for the two considered groups showing characteristics of MC and BDE. The last row corresponds to the arithmetic mean of V_{ICME}, with the standard deviation as uncertainty.

	kmTII-ICMEs	other-ICMEs
MC (%)	34	39
BDE (%)	74	48
$\bar{V}_{ICME}$ [km s^{-1}]	545 ± 163	442 ± 97

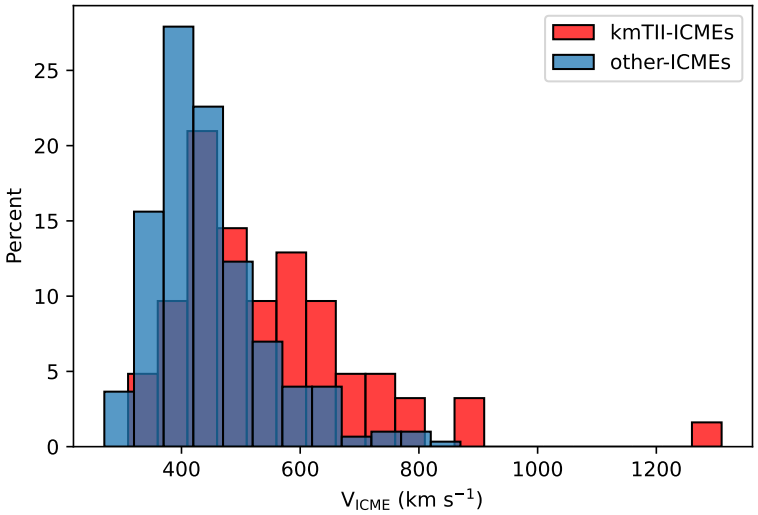

Figure 3. Histograms of (V_{ICME}) for both groups of analysis. Given the difference in number of events, a percent normalization was used, such that bar heights sum to 100.

53. This result indicates that, if considering the mean values, the DsT of those ICMEs associated with kmTII emission is twice as large (in negative values) than that of those ICMEs not associated with kmTII.

In Figure 4 we present a plot of DsT versus the mean speed of the associated ICMEs. The figure suggests that for both considered groups, faster ICMEs are related with the occurrence of stronger geomagnetic storms (characterized by higher DsT in absolute value; Gopalswamy, 2009). However, the linear correlation between DsT and V_{ICME} is weak, on the basis of the correlation coefficients for both data series.

To specifically analyze those ICMEs associated to moderate and intense geomagnetic storms (Gonzalez, Tsurutani, and Clúa de Gonzalez, 1999), we considered only those events whose DsT ≤ -50 (Loewe and Prölss, 1997). With this consideration, we found that out of the 62 events of the group kmTII-ICMEs, 49 (79%) produced moderate to intense geomagnetic storms. These events present a mean DsT value of -133, with a median of -105. The other-ICMEs group, originally comprised of 302 events, was left

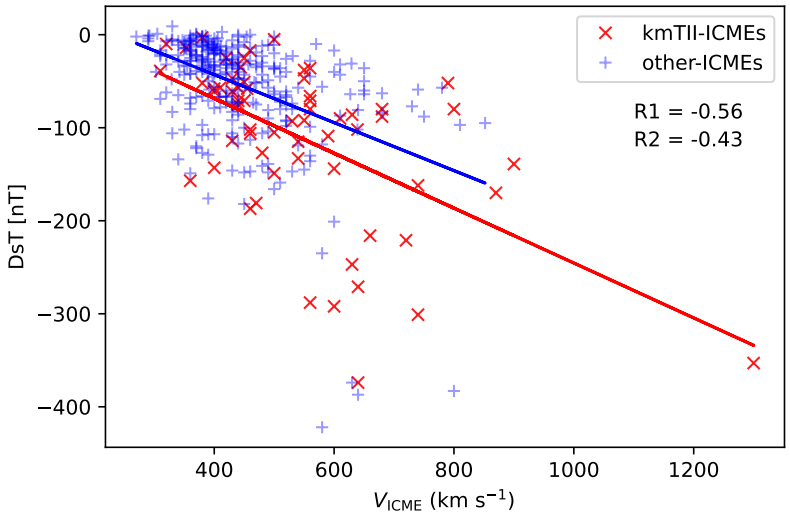

Figure 4. DsT values vs. V_{ICME}, for all considered events in the kmTII-ICMEs and other-ICMEs groups. Linear fits are displayed in the same color than its group. The linear correlation coefficient R1 corresponds to kmTII-ICMEs and R2 to other-ICMEs.

with 115 (38%) after removing those events with DsT > -50. For this group we found a mean DsT value of -102, with a median of -81. These results suggest that kmTII-related ICMEs are more prone to produce larger geomagnetic storms. In fact, these are up to 25% larger than for those ICMEs not linked to kmTII emission events. This is in agreement with Patel et al. (2022), who also found that decametric and hectometric type II-related ICMEs produced more intense geomagnetic storms, with faster ICMEs on average. Moreover, we also find that the proportion of ICMEs producing moderate to intense geomagnetic storms is twice as large for the kmTII-ICMEs group than for the other-ICMEs group (79% vs. 38% respectively).

5. Discussion and conclusions

According to the identification criteria adopted in this work, we compiled a list of 134 kmTII events on the basis of TNR data during the years 2000 – 2012. We searched for associations amongst the 134 radio events in our list with interplanetary transient phenomena detected in-situ at 1 AU, such as shockwaves and ICMEs reported by existing catalogs. Following temporal and spatial considerations, it was possible to associate 57% of the kmTII events to a shockwave and 46% to an ICME. Of particular importance is the finding of 45 kmTII events out of of the total 134 (33%) which had not been reported by the official Wind/WAVES catalog (based on RAD1 and RAD2 data).

We analyzed the solar cycle variation of all kmTIIs, with associated shock and ICMEs. We find that, for the maximum of solar cycle 23, the amount of shock-associated kmTIIs is notably larger than half of the total kmTIIs, while for the other epochs this

proportion is lower. KmTIIs associated with both shocks and ICMEs represent typically less than half of the total KmTIIs, except for the year 2002. During the years 2008 – 2010 no kmTIIs were found, in accordance with the yearly number of shocks which significantly decreases during those years. This is however not the case for the amount of ICMEs detected near Earth, which notably starts increasing from 2008 onwards (see Figure 2).

ICMEs with (kmTII-ICMEs) and without (other-ICMEs) associated KmTIIs were compared in regards to their main characteristics. Regarding the mean speed of ICMEs, kmTII-ICMEs are 23% faster on average than the other-ICMEs. This is consistent with the fact that low frequency radio bursts are associated with faster CMEs on average (Patel et al., 2022). As for the fraction of ICMEs classified as MCs, it is roughly similar for both groups of ICMEs. However, the proportion of ICMEs with BDEs is noticeably different, with 74% of the KmTII-ICMEs group having BDEs vs. 48% for the other-ICMEs group. Note that the presence of BDEs suggests that electrons are mirroring within closed magnetic structures with both ends anchored at the Sun's surface or disconnected plasmoids (Gosling, 1990; Carcaboso et al., 2020).

The analysis of DsT values for both ICME groups yields that, for the kmTII-ICMEs the mean value is twice as large than for the other-ICMEs group (-111 vs. -53). This implies that kmTIIs-ICMEs produce intense storms on average, as opposite to the other-ICMEs, which tend to produce moderate storms. When considering events with Dst $<$ -50, the storms produced by kmTII-ICMEs are 25% larger than those from other-ICMEs (-133 vs. -102). Moreover, the proportion of ICMEs producing moderate to intense geomagnetic storms is twice as large for the kmTII-ICMEs group than for the other-ICMEs group (79% vs. 38%).

With regards to the differences between the number of kmTIIs compiled in our list and Wind's list, it is worth noting that the latter reports some events to reach frequencies lower than 300 kHz that could not be identified in the TNR dynamic spectra during our survey. Some of them were even associated to structures detected in-situ at Earth. One of the possible reasons to this issue might have been that the missing kmTII events are hidden behind other radio structures in the DS, especially for solar maximum times. On the other hand, it is also plausible that the lower resolution of RAD1 at the bottom end of its frequency range may lead to misleading inferences.

We report here on 45 new kmTII events not reported by the official Wind/WAVES catalog, which is built on the basis of RAD1 and RAD2 data. While about a third of the 45 new kmTIIs do have an apparent higher frequency counterpart, the remaining events do not. This finding poses new open questions on these low frequency TII radio bursts, regarding their generation mechanisms and the circumstances that favour their detection. It is plausible either that these new events are primarily composed of bursts that only started emitting below the frequency range of RAD1, or that they have traveled relatively unencumbered until meeting some density structure in interplanetary space. Another explanation to this finding is that kmTII emissions are wider-beamed than shorter-wavelength emissions, thus enabling their detection even if the main propagation direction of the shock is far off the Sun-Earth line.

Given that kmTIIs are closely related to the presence of shockwaves in the IP medium, it is expected that most of the kmTIIs identified in this work can be succesfully associated to a shockwave. However, this was not the case for 42% of the kmTIIs. This can be explained, at least partially, by the following:

- The shock has indeed arrived but for some reason it was not detected and/or cataloged as such. The increase in the quantities that define the presence of a shock may have smoothed or somewhat diffused in the background solar wind and is too weak to be detected at 1 AU.
- In spite of the kmTII being detected by Wind/WAVES, the shock is not precisely travelling in the direction of the spacecraft, i.e. the portion of the shockwave that produced the kmTII is not on the Sun-Earth line.

Inspired by the fact that for some of the kmTIIs lacking a reported shock in the inspected catalogs, it was still possible to infer the presence of a shock in the DS, we took a closer look at some events. In particular, for the ICMEs that produced kmTIIs but do not have associated shocks according to the inspected catalogs, we searched for shocks directly in the data. Those 11 events (Table 1) were analyzed on a case by case basis, considering magnetic field, flow speed, proton density and flow pressure. After this inquiry, we found evidence of a shock matching the ICME date of arrival for at least 9 of those 11 events. Only for 2 events we did not find any evidence of a shock. This suggests that a shock might have been responsible of the kmTII generation in most of the cases, but its properties have somewhat subsided. Therefore, it is plausible that smoothing/diffusion processes might be the reason that the ratio of kmTII associated shocks against kmTII emissions is not constant over the solar cycle.

The results of this investigation reinforce the importance of using data from TNR to identify kmTII events propagating in the interplanetary medium that cannot be detected by the other receivers of Wind/WAVES. In fact, from the 45 newly reported kmTII events, 23 are associated to an in-situ shockwave. Considering that these low-frequency radio emissions can be used as a predictor for shock arrival time at Earth with an average error of $\approx$ 4 h (Cremades et al., 2015), the amount of events for which space weather forecasts can be improved is increased.

Acknowledgements FM is fellow of CONICET. HC and FML are members of the Carrera del Investigador Científico (CONICET). TNC acknowledges that this work falls within the objectives of LASSOS. The authors thank E. Aguilar-Rodríguez for his disinterested support on SolarSoft routines for DS generation. The authors acknowledge the use of data from the Wind (NASA) mission, as well as in situ data courtesy of N. Ness at Bartol Research Institute; D.J. McComas at SWRI; J.H. King and N. Papatashvilli at AdnetSystems NASA GSFC, and CDAWeb.

Appendix

A. Complete table of identified events

Table 3.: List of the 134 identified kmTII events, their associations with shocks and ICMEs, and main characteristics. Columns (1-2): kmTII start date and time. (3-4) kmTII end date and time. (5) kmTII frequency range as measured in TNR's DS [kHz]. Reminder that TNR's maximum frequency of observation is 256 kHz, so some kmTII may continue up to higher frequencies in the other receivers. (6) Year and reference number for the detection made by Wind/WAVES list. (7-8) Shock start date and time. (9) Shock speed [km s^{-1}]. (10) Shock catalog. (11-12) ICME start date and time. (13) MC type, according to RC list (see Section 3 for details). (14) Magnetic obstacle type, according to TNC catalog (see Section 3). (15) Existence of bidirectional suprathermal electron strahls. (16) Maximum solar wind speed during the passage of the ICME [km s^{-1}]. (17) Mean magnetic field value during the ICME interval [nT]. (18) Minimum DsT value during the ICME passage [nT]. (19) ICME catalogs for which an association was found. All times are in UTC.

KmTII					Wind/WAVES	In situ shock				ICME								
Start date & time		End date & time		Freq. range	Year/Ref	Start date & time		Speed	Catalog	Start date & time		MC	MO	BDE	V_{ICME}	B	DsT	Catalog
(1)	(2)	(3)	(4)	(5)	(6)	(7)	(8)	(9)	(10)	(11)	(12)	(13)	(14)	(15)	(16)	(17)	(18)	(19)
20000109	1500	20000110	1800	245-58	2000/1	20000111	1340	514.4	ace									
20000129	0630	20000129	1930	200-40	2000/5	20000130	1844	642.9	ace									
20000208	2000	20000210	0400	200-27	2000/7													
20000210	1800	20000211	0000	47-37		20000211	0212	549.9	wind/ace	20000211	0258	0		Y	420	7	-25	RC
20000211	0830	20000211	2330	55-25	2000/9	20000211	2334	638.3	wind/ace	20000211	2352	2	Fr	Y	540	13	-133	RC/TNC
20000310	0030	20000312	0300	166-33	2000/15													
20000317	0600	20000318	0030	77-25	2000/16					20000318	2200	0		Y	380	9	-3	RC
20000406	0000	20000406	1300	240-100	2000/22	20000406	1632	641.5	wind	20000406	1639	1		Y	560	6	-288	RC
20000516	0440	20000516	1400	166-50	2000/38					20000516	2300	1		N	550	9	-92	RC
20000607	0200	20000607	1300	245-50	2000/41	20000608	0841	868.7	ace	20000608	0910	0	E	Y	610	11	-90	RC/TNC
20000714	1300	20000715	0600	200-30	2000/57					20000715	1437	2	F+	Y	740	20	-301	RC/TNC
20000716	1300	20000716	2200	245-100	2000/59	20000719	1530	638.2	wind	20000719	1527	0	Cx	Y	530	8	-93	RC/TNC
20000726	0900	20000727	0400	200-66	2000/66	20000728	0542	474.7	ace	20000728	0634	2	F+	Y	440	9	-71	RC/TNC
20000905	0300	20000905	1100	90-50	2000/67	20000906	1613	539.9	ace	20000906	1702		Cx		444	8.93	-35	TNC
20000913	0700	20000913	1230	200-58	2000/68													
20000914	0845	20000914	2130	77-38		20000915	0427	374.7	wind									
20000930	1300	20001001	2130	200-50	2000/74	20001003	0102		wind	20001003	0054	2	F+	Y	400	14	-143	RC/TNC

Table 3 – continued from previous page

Km Type II					Wind/WAVES	In situ shock				ICME								
Start date & time		End date & time		Freq. range	Year/Ref	Start date & time		Speed	Catalog	Start date & time		MC	MO	BDE	V_{ICME}	B	DsT	Catalog
(1)	(2)	(3)	(4)	(5)	(6)	(7)	(8)	(9)	(10)	(11)	(12)	(13)	(14)	(15)	(16)	(17)	(18)	(19)
20001015	1200	20001016	2300	100-37	2000/77													
20001029	0600	20001030	0300	200-60	2000/81	20001031	1630	480.5	ace									
20001101	0330	20001102	1200	83-58	2000/82	20001102	2347	279.0	UNH									
20001110	0015	20001110	1500	240-55	2000/85	20001111	0412	964.8	wind/ace	20001111	0411		E	N	790	7	-52	TNC
20001124	1100	20001124	1500	200-100	2000/93													
20001124	2100	20001126	0800	240-28		20001126	1143	524.4	wind/ace	20001126	1158	0	Fr	Y	560	10	-80	RC/TNC
20010110	0500	20010111	1300	0-25	2001/2													
20010112	0000	20010113	0000	77-32	2001/3	20010113	0225	398.0	wind/ace									
20010115	1300	20010115	1930	200-66	2001/4	20010117	1622	422.6	wind									
20010118	2100	20010119	0300	100-62	2001/5													
20010122	1700	20010123	0545	59-35		20010123	1049	615.3	wind/ace	20010123	1048	1	Cx	Y	400	4	-61	RC/TNC
20010130	0000	20010130	1800	77-35		20010131	0835	486.5	wind/ace									
20010329	1800	20010329	2230	240-60	2001/17	20010330	2151	357.1	ace									
20010331	0200	20010401	1730	200-43														
20010407	0630	20010407	1715	240-0	2001/22	20010407	1756	604.3	wind/ace									
20010409	1930	20010410	0040	200-83	2001/24													
20010410	1200	20010411	0600	200-33		20010411	1314	560.5	ace	20010411	1343	2	F-	Y	640	14	-271	RC/TNC
20010416	0000	20010416	0630	245-100	2001/27	20010418	0049	601.2	wind	20010418	0046	0		Y	430	8	-114	
20010418	0900	20010418	1420	200-111	2001/28													
20010424	1700	20010425	0630	66-40	2001/29													
20010427	0300	20010428	0500	200-20	2001/30	20010428	0500	930.1	wind	20010428	0501	2	Cx	N	550	8	-47	RC/TNC
20010504	0530	20010504	0730	125-100	2001/31	20010506	0906	347.2	wind									
20010611	1100	20010612	0700	200-59	2001/34													
20010615	0630	20010615	1015	220-58	2001/35													
20010618	1800	20010619	1800	245-71	2001/39													
20010720	0140	20010720	0630	166-71	2001/40													

Table 3 – continued from previous page

Km Type II					Wind/WAVES	In situ shock				ICME								
Start date & time		End date & time		Freq. range	Year/Ref	Start date & time		Speed	Catalog	Start date & time		MC	MO	BDE	V_{ICME}	B	DsT	Catalog
(1)	(2)	(3)	(4)	(5)	(6)	(7)	(8)	(9)	(10)	(11)	(12)	(13)	(14)	(15)	(16)	(17)	(18)	(19)
20010810	1400	20010810	1930	125-83	2001/41	20010812	1109	419.1	wind/ace									
20010816	1500	20010816	2230	240-66	2001/42	20010817	1101	519.1	wind/ace	20010817	1103	0	F-	Y	500	11	-105	RC/TNC
20010825	2100	20010826	1100	240-100	2001/43													
20010912	1000	20010912	1530	142-77	2001/46	20010913	0231	449.3	wind	20010913	0231	1		Y	410	10	-57	RC
20010913	1700	20010914	0330	200-110	2001/47													
20010924	1230	20010925	2000	245-30	2001/54	20010925	2017	850.6	wind	20010925	2016		F-		639	14.12	-102	TNC
20010927	1400	20010927	2300	245-90	2001/55	20010929	0929	725.1	wind	20010929	0940	1	Cx	Y	560	12	-66	RC/TNC
20011010	1115	20011010	2200	143-50	2001/61	20011011	1650	579.0	wind/ace	20011011	1701	1		Y	560	22	-71	RC
20011020	0600	20011021	1600	240-33	2001/63	20011021	1640	636.0	wind/ace	20011021	1648	0	Fr	Y	460	9	-187	RC/TNC
20011024	0300	20011024	2045	62-33		20011025	0859	366.9	wind/ace									
20011026	0000	20011027	2330	240-30	2001/65	20011028	0313	589.1	wind	20011028	0319	0	E	N	360	5	-157	RC/TNC
20011028	1700	20011028	2215	166-100	2001/66													
20011104	2100	20011106	0100	245-35		20011106	0125		UNH	20011106	0152	1		Y	600	7	-292	RC
20011107	1900	20011108	0800	166-50														
20011117	1600	20011118	0400	200-66	2001/72	20011119	1815	628.9	wind/ace	20011119	1815	1		Y	430	6	-47	RC
20011123	0530	20011124	0400	245-30	2001/75	20011124	0454	658.7	wind	20011124	0656	2	Fr	Y	720	14	-221	RC/TNC
20011226	1100	20011227	0300	240-90	2001/78	20011229	0517	527.4	wind/ace	20011229	0538	1	Fr	N	400	16	-58	RC/TNC
20020214	0600	20020214	1400	245-200	2002/5	20020217	0124	300.9	wind/ace									
20020311	1030	20020314	1000	181-62														
20020412	0400	20020415	2300	91-43														
20020416	1500	20020416	2300	142-83		20020417	1101	516.8	wind/ace	20020417	1107	2	F+	Y	480	14	-127	RC/TNC
20020417	1330	20020419	0130	240-50	2002/17	20020419	0825	768.4	wind/ace	20020419	0835	2	Fr	Y	500	8	-149	RC/TNC
20020421	0800	20020421	2400	240-43	2002/19	20020423	0500	644.2	wind/ace									
20020508	0115	20020508	1845	100-43		20020510	1029	431.3	ace	20020510	1109		Fr		353	6.84	-14	TNC
20020517	0800	20020518	1000	125-42		20020518	1945	545.0	wind/ace	20020518	1945		Fr		455	11.20	-58	TNC
20020522	1600	20020523	1000	200-0	2002/25	20020523	1015	770.6	wind/ace	20020523	1050	2	F-	Y	590	11	-109	RC/TNC

Table 3 – continued from previous page

Km Type II					Wind/WAVES	In situ shock				ICME								
Start date & time		End date & time		Freq. range	Year/Ref	Start date & time		Speed	Catalog	Start date & time		MC	MO	BDE	V_{ICME}	B	DsT	Catalog
(1)	(2)	(3)	(4)	(5)	(6)	(7)	(8)	(9)	(10)	(11)	(12)	(13)	(14)	(15)	(16)	(17)	(18)	(19)
20020524	2300	20020525	1730	143-45														
20020716	0330	20020716	1600	240-40	2002/29	20020717	1555	483.2	wind	20020717	1603	1	Fr	Y	460	6	-17	RC/TNC
20020730	0200	20020801	1200	166-45		20020801	0424	446.5	ace	20020801	0510	2	Fr	N	450	12	-51	RC/TNC
20020731	1200	20020801	2300	125-83		20020801	2309	495.5	wind	20020801	2309	2	Fr	Y	460	10	-102	RC/TNC
20020817	1130	20020817	2000	220-50	2002/41	20020818	1840	671.5	wind	20020818	1846	1	Fr	Y	460	8	-106	RC/TNC
20020824	0700	20020824	1240	250-71		20020826	1041	400.0	UNH									
20020906	0000	20020907	0800	250-31	2002/43	20020907	1622	897.0	wind/ace	20020907	1636	0		Y	470	11	-181	RC
20021115	0410	20021115	1830	230-59		20021116	2304	514.3	ace	20021116	2305	1	F-	Y	380	10	-52	RC/TNC
20021219	1000	20021220	1700	100-42						20021220	1700	0	Fr	N	440	11	-75	RC/TNC
20030201	0230	20030201	2030	245-30														
20030319	2330	20030320	0930	100-35														
20030528	1000	20030529	0100	245-50	2003/14	20030529	1831	906.6	ace	20030529	1825	1		Y	600	20	-144	RC
20031023	0100	20031023	23:59	170-71						20031024	1524	1		Y	560	21	-36	RC
20031028	0600	20031029	0600	38-21	2003/26					20031029	0611	2	Cx	Y	1300	32	-353	RC/TNC
20031103	0430	20031103	1930	200-43		20031104	0646	759.0	wind									
20031104	2230	20031105	1800	240-38														
20040725	2330	20040726	2200	180-22	2004/15	20040726	2225	1086.3	wind/ace	20040726	2249	2	Cx	Y	870	16	-170	RC/TNC
20040729	1930	20040730	1815	250-35	2004/18	20040730	2031	573.7	ace									
20040812	0315	20040812	0930	200-100														
20040913	0000	20040913	1930	140-35	2004/21					20040913	2003	1	E	Y	550	6	-38	RC/TNC
20041105	0230	20041105	2300	66-31														
20041107	2200	20041108	1930	240-30	2004/30	20041109	1825	812.9	wind	20041109	1825	2	F+	SEP	640	14	-374	RC/TNC
20041203	0700	20041204	9999	180-100	2004/36													
20050116	0300	20050117	0600	250-40	2005/4	20050117	0715	651.8	ace									
20050117	1300	20050118	1400	250-43	2005/6					20050118	2100	0	F-	Y	800	12	-80	RC/TNC
20050212	1400	20050213	0900	180-60														

Table 3 – continued from previous page

Km Type II					Wind/WAVES	In situ shock				ICME								
Start date & time		End date & time		Freq. range	Year/Ref	Start date & time		Speed	Catalog	Start date & time		MC	MO	BDE	V_{ICME}	B	DsT	Catalog
(1)	(2)	(3)	(4)	(5)	(6)	(7)	(8)	(9)	(10)	(11)	(12)	(13)	(14)	(15)	(16)	(17)	(18)	(19)
20050513	2130	20050515	0210	200-27	2005/18	20050515	0210	857.5	wind	20050515	0238	2	F+	Y	630	15	-247	RC/TNC
20050723	1700	20050724	1400	240-111														
20050724	1530	20050724	2200	240-140	2005/29													
20050730	1130	20050801	0100	250-0	2005/32	20050801	0600	479.6	wind									
20050822	0800	20050824	0530	250-38	2005/36	20050824	0535	566.3	wind/ace	20050824	0613	1		Y	660	20	-216	RC
20050909	2100	20050910	0900	240-90	2005/44	20050911	0057	1146.6	wind	20050911	0114	0		Y	900	10	-139	RC
20050912	2200	20050913	0615	90-43						20050913	0900	0		Y	630	5	-86	RC
20050913	1200	20050913	1930	166-83	2005/48													
20050914	0430	20050915	0515	200-34		20050915	0836/0839	663.9	wind/ace	20050915	0600	1		Y	680	7	-80	RC
20050915	1700	20050916	0830	125-25	2005/50													
20060817	0030	20060817	0500	200-140		20060818	1548	497.8	wind									
20061202	1350	20061202	2400	200-77														
20061206	2130	20061207	0700	250-25	2006/10													
20061213	0820	20061213	2340	250-70	2006/11	20061214	1351	1011.9	wind/ace	20061214	1414	2	F-	Y	740	13	-162	RC/TNC
20070125	0013	20070125	2330	250-70	2007/1													
20110415	1930	20110417	2100	200-59		20110418	0546	369.6	wind									
20110530	0400	20110530	1000	200-100	2011/14													
20110616	0130	20110617	0200	66-20						20110617	0241	1	Cx	Y	500	9	-5	RC/TNC
20110804	0700	20110805	1730	240-26	2011/23	20110805	1732	411.7	wind	20110805	1751	1		Y	540	4	-115	RC
20110809	2230	20110810	2300	245-30														
20110922	1600	20110924	1800	245-30	2011/31	20110925	1046	265.6	wind									
20111022	1800	20111023	0600	200-40	2011/40													
20111126	1200	20111128	0500	145-35	2011/43	20111128	2100	454.8	wind	20111128	2150	2	Cx	Y	450	15	-25	RC/TNC
20120119	1900	20120121	9999	0	2012/2	20120121	0402	325.4	wind	20120121	0501	2	Fr	N	320	10	-10	RC/TNC
20120121	1700	20120121	2400	55-35		20120122	0533	442.8	wind	20120122	0611	2	F-	Y	450	9	-71	RC/TNC
20120123	0700	20120124	1430	245-20	2012/3	20120124	1440	735.8	wind									

Table 3 – continued from previous page

Km Type II					Wind/WAVES	In situ shock				ICME								
Start date & time		End date & time		Freq. range	Year/Ref	Start date & time		Speed	Catalog	Start date & time		MC	MO	BDE	V_{ICME}	B	DsT	Catalog
(1)	(2)	(3)	(4)	(5)	(6)	(7)	(8)	(9)	(10)	(11)	(12)	(13)	(14)	(15)	(16)	(17)	(18)	(19)
20120127	2200	20120128	0800	245-65	2012/4	20120130	1543	356.5	wind									
20120224	2330	20120226	1200	245-30	2012/6					20120226	2139	2	Cx	Y	440	13	-57	RC/TNC
20120307	0300	20120309	0800	245-30	2012/11													
20120310	2300	20120311	1100	245-50	2012/13													
20120314	0500	20120314	1200	240-27		20120315	1230	650.0	UNH	20120315	1306	1	Fr	N	680	9	-88	RC/TNC
20120420	2115	20120420	2400	245-58														
20120517	0530	20120517	1930	245-80														
20120708	1900	20120710	2030	245-35														
20120710	1530	20120712	1600	165-40														
20120717	2345	20120718	0545	200-100	2012/39	20120720	0430	440.0	UNH									
20120901	1500	20120902	2200	100-30		20120903	1121	428.6	wind	20120903	1213	0		-	430		-61	RC
20120920	0200	20120920	0530	200-142	2012/49													
20120928	1400	20120929	1300	240-45		20120930	1014	338.2	wind	20120930	1131	0	Cx	-	310	8	-39	RC/TNC

Author Contribution All authors contributed to the study conception and design. Material preparation, data collection and analysis were performed by FM under the guidance of HC and FML. The first draft of the manuscript was written by FM and all authors commented on previous versions of the manuscript. All authors read and approved the final manuscript.

Funding This work is supported by projects PIP112202001027l0CO (CONICET) and MSTCAME0008181TC (UTN).

Data Availability The datasets generated and analyzed during the current study are available from the corresponding author on reasonable request. The KmTII list is available at this link: https://sites.google.com/um.edu.ar/gehme/science/km-tii-catalogue.

Conflict of interest The authors declare that they have no conflicts of interest.

References

Aguilar-Rodriguez, E., Gonzalez-Esparza, A., Ontiveros, V.: 2010, Tracking of Interplanetary CME/Shocks evolution using Type II radio burst observations. In: *AGU Fall Meeting Abstracts* **2010**, SH23B. ADS.

Bale, S.D., Reiner, M.J., Bougeret, J.-L., Kaiser, M.L., Krucker, S., Larson, D.E., Lin, R.P.: 1999, The source region of an interplanetary type II radio burst. *grl* **26**, 1573. DOI. ADS.

Bougeret, J.-L., Kaiser, M.L., Kellogg, P.J., Manning, R., Goetz, K., Monson, S.J., Monge, N., Friel, L., Meetre, C.A., Perche, C., Sitruk, L., Hoang, S.: 1995, Waves: The Radio and Plasma Wave Investigation on the Wind Spacecraft. *Space Science Reviews* **71**, 231. DOI. ADS.

Cane, H.V., Erickson, W.C.: 2005, Solar Type II Radio Bursts and IP Type II Events. *The Astrophysical Journal* **623**, 1180. DOI. ADS.

Cane, H.V., Richardson, I.G.: 2003, Interplanetary coronal mass ejections in the near-Earth solar wind during 1996-2002. *Journal of Geophysical Research (Space Physics)* **108**, 1156. DOI. ADS.

Cane, H.V., Sheeley, J. N. R., Howard, R.A.: 1987, Energetic interpanetary shocks, radio emission, and coronal mass ejections. *Journal of Geophysical Research* **92**, 9869. DOI. ADS.

Cane, H.V., Stone, R.G., Fainberg, J.: 1982, Type II solar radio events observed in the interplanetary medium. *Sol Phys* **78**, 187–198. DOI.

Carcaboso, F., Gómez-Herrero, R., Espinosa Lara, F., Hidalgo, M.A., Cernuda, I., Rodríguez-Pacheco, J.: 2020, Characterisation of suprathermal electron pitch-angle distributions - Bidirectional and isotropic periods in solar wind. *A&A* **635**, A79. DOI. https://doi.org/10.1051/0004-6361/201936601.

Chernov, G., Fomichev, V.: 2021, On the Issue of the Origin of Type II Solar Radio Bursts. *The Astrophysical Journal* **922**, 82. DOI. ADS.

Corona-Romero, P., Gonzalez-Esparza, J.A., Aguilar-Rodriguez, E., De-la-Luz, V., Mejia-Ambriz, J.C.: 2015, Kinematics of ICMEs/Shocks: Blast Wave Reconstruction Using Type-II Emissions. *Solar Physics* **290**, 2439. DOI. ADS.

Cremades, H., St. Cyr, O.C., Kaiser, M.L.: 2007, A tool to improve space weather forecasts: Kilometric radio emissions from Wind/WAVES. *Space Weather* **5**, S08001. DOI. ADS.

Cremades, H., Iglesias, F.A., St. Cyr, O.C., et al.: 2015, Low-Frequency Type-II Radio Detections and Coronagraph Data Employed to Describe and Forecast the Propagation of 71 CMEs/Shocks. *Sol. Phys.* **2455**.

Dulk, G.A., Leblanc, Y., Bougeret, J.-L.: 1999, Type II shock and CME from the corona to 1 AU. *Geophysical Research Letters* **26**, 2331. DOI. https://agupubs.onlinelibrary.wiley.com/doi/abs/10.1029/1999GL900454.

Gonzalez, W.D., Tsurutani, B.T., Clúa de Gonzalez, A.L.: 1999, Interplanetary origin of geomagnetic storms. *Space Science Reviews* **88**, 529. DOI. ADS.

Gonzalez-Esparza, A., Aguilar-Rodriguez, E.: 2009a, Speed evolution of fast CME/shocks with SOHO/LASCO, WIND/WAVES, IPS and in-situ WIND data: analysis of kilometric type-II emissions. *Annales Geophysicae* **27**, 3957. DOI. ADS.

Gonzalez-Esparza, A., Aguilar-Rodriguez, E.: 2009b, Speed evolution of fast CME/shocks with SOHO/LASCO, WIND/WAVES, IPS and in-situ WIND data: analysis of kilometric type-II emissions. *Annales Geophysicae* **27**, 3957. DOI. ADS.

Gopalswamy, N.: 2009, The CME link to geomagnetic storms. *Proceedings of the International Astronomical Union* **264**. DOI.

Gopalswamy, N., Mäkelä, P., Yashiro, S.: 2019, A Catalog of Type II radio bursts observed by Wind/WAVES and their Statistical Properties. *Sun and Geosphere* **14**, 111. DOI. ADS.

Gopalswamy, N., Yashiro, S., Akiyama, S., Mäkelä, P., Xie, H., Kaiser, M.L., Howard, R.A., Bougeret, J.L.: 2008, Coronal mass ejections, type II radio bursts, and solar energetic particle events in the SOHO era. *Annales Geophysicae* **26**, 3033. DOI. https://angeo.copernicus.org/articles/26/3033/2008/.

Gosling, J.T.: 1990, Coronal mass ejections and magnetic flux ropes in interplanetary space. *Physics of magnetic flux ropes* **58**, 343.

Hillan, D.S., Cairns, I.H., Robinson, P.A.: 2012, Type II solar radio bursts: 2. Detailed comparison of theory with observations. *Journal of Geophysical Research: Space Physics* **117**. DOI. https://agupubs.onlinelibrary.wiley.com/doi/abs/10.1029/2011JA016755.

Kaiser, M.L., Reiner, M.J., Gopalswamy, N., Howard, R.A., St. Cyr, O.C., Thompson, B.J., Bougeret, J.-L.: 1998, Type II radio emissions in the frequency range from 1–14 MHz associated with the April 7, 1997 solar event. *Geophysical Research Letters* **25**, 2501. DOI. https://agupubs.onlinelibrary.wiley.com/doi/abs/10.1029/98GL00706.

Knock, S.A., Cairns, I.H., Robinson, P.A., Kuncic, Z.: 2001, Theory of type II radio emission from the foreshock of an interplanetary shock. *Journal of Geophysical Research: Space Physics* **106**, 25041. DOI. https://agupubs.onlinelibrary.wiley.com/doi/abs/10.1029/2001JA000053.

Leblanc, Y., Dulk, G.A., Bougeret, J.-L.: 1998, Tracing the Electron Density from the Corona to 1au. *Solar Physics* **183**, 165. DOI. ADS.

Loewe, C.A., Prölss, G.W.: 1997, Classification and mean behavior of magnetic storms. *Journal of Geophysical Research: Space Physics* **102**, 14209. DOI. https://agupubs.onlinelibrary.wiley.com/doi/abs/10.1029/96JA04020.

Malitson, H., Fainberg, J., Stone, R.: 1973, Observation of a Type II Solar Radio Burst to 37 R&sun. *Astrophysical Letters* **14**, 111.

Nieves-Chinchilla, T., Vourlidas, A., Raymond, J., Linton, M., Al-Haddad, N., Savani, N., Szabo, A., Hidalgo, M.: 2018, Understanding the Internal Magnetic Field Configurations of ICMEs Using More than 20 Years of Wind Observations. *Sol. Phys.* **293**, 27. ISBN 978-94-024-1569-8. DOI.

Nieves-Chinchilla, T., Jian, L.K., Balmaceda, L., Vourlidas, A., dos Santos, L.F.G., Szabo, A.: 2019, Unraveling the Internal Magnetic Field Structure of the Earth-directed Interplanetary Coronal Mass Ejections During 1995-2015. *Sol. Phys.* **294:84**. DOI.

Patel, B.D., Joshi, B., Cho, K.-S., Kim, R.S., Moon, Y.: 2022, Near-Earth Interplanetary Coronal Mass Ejections and Their Association with DH Type II Radio Bursts During Solar Cycles 23 and 24. *Solar Physics* **297**.

Reiner, M.J., Kaiser, M.L., Bougeret, J.-L.: 2007, Coronal and Interplanetary Propagation of CME/Shocks from Radio, In Situ and White-Light Observations. *The Astrophysical Journal* **663**, 1369. DOI. https://dx.doi.org/10.1086/518683.

Reiner, M.J., Kaiser, M.L., Fainberg, J., Bougeret, J.-L., Stone, R.G.: 1997, Remote Radio Tracking of Interplanetary CMEs. In: Wilson, A. (ed.) *Correlated Phenomena at the Sun, in the Heliosphere and in Geospace*, *ESA Special Publication* **415**, 183. ADS.

Reiner, M.J., Kaiser, M.L., Fainberg, J., Stone, R.G.: 1998, A new method for studying remote type II radio emissions from coronal mass ejection-driven shocks. *Journal of Geophysical Research: Space Physics* **103**, 29651. DOI. https://agupubs.onlinelibrary.wiley.com/doi/abs/10.1029/98JA02614.

Richardson, I.G., Cane, H.V.: 2010, Near-Earth Interplanetary Coronal Mass Ejections During Solar Cycle 23 (1996-2009): Catalog and Summary of Properties. *Sol. Phys.* **264**, 189. DOI. ADS.

Wild, J., LL., M.: 1950, Observatioas of the Spectrum of High-Intensity Solar Radiation at Metre Wavelengths. I. The Apparatus and Spectral Types of Solar Burst Observed. *Australian Journal of Chemistry* **3**, 387. DOI.

Wild, J., Murray, J., Rowe, W.: 1954, Harmonics in the Spectra of Solar Radio Disturbances. *Australian Journal of Physics* **7**, 439. DOI.

Xie, H., Odstrcil, D., Mays, L., St. Cyr, O.C., Gopalswamy, N., Cremades, H.: 2012, Understanding shock dynamics in the inner heliosphere with modeling and Type II radio data: The 2010-04-03 event. *Journal of Geophysical Research (Space Physics)* **117**, A04105. DOI. ADS.